---

**Article:**
Cordara, T., Smith, H., Mohun, R. orcid.org/0000-0003-1125-5802 et al. (4 more authors) (2020) Hot Isostatic Pressing (HIP): A novel method to prepare Cr-doped UO2 nuclear fuel. MRS Advances, 5 (1-2). pp. 45-53. ISSN 2059-8521

https://doi.org/10.1557/adv.2020.62

---

MRS Advances

# Hot Isostatic Pressing (HIP): A novel method to prepare Cr-doped $UO_2$ nuclear fuel

Theo Cordara, Hannah Smith, Ritesh Mohun, Laura J. Gardner, Martin C. Stennett, Neil C. Hyatt and Claire L. Corkhill*

*NucleUS Immobilisation Science Laboratory, Department of Materials Science and Engineering, University of Sheffield, Sheffield, S1 3JD, United Kingdom*

*ABSTRACT*

*The addition of $Cr_2O_3$ to modern $UO_2$ fuel modifies the microstructure so that, through the generation of larger grains during fission, a higher proportion of fission gases can be accommodated. This reduces the pellet-cladding mechanical interaction of the fuel rods, allowing the fuels to be "burned" for longer than traditional $UO_2$ fuel, thus maximising the energy obtained. We here describe the preparation of $UO_2$ and Cr-doped $UO_2$ using Hot Isostatic Pressing (HIP), as a potential method for fuel fabrication, and for development of analogue materials for spent nuclear fuel research. Characterization of the synthesised materials confirmed that high density $UO_2$ was successfully formed, and that Cr was present as particles at grain boundaries and also within the $UO_2$ matrix, possibly in a reduced form due to the processing conditions. In contrast to studies of Cr-doped $UO_2$ synthesised by other methods, no significant changes to the grain size were observed in the presence of Cr.*

## INTRODUCTION

Recent media coverage of the Hinkley Point C nuclear power station in the UK has highlighted the extreme costs of generating energy through nuclear fission in light water reactors (LWR). One way that power producers have sought to lower the cost is by developing new fuels that are capable for being "burnt" for longer within the reactor, maximising the amount of energy obtained from each fuel pellet and increasing the flexibility and reliability of LWR fuel [1]. One of the main limitations for how long fuel can remain in the reactor is the ability of the fuel to accommodate fission products, especially fission gases such as Kr, Xe, He, etc. The build-up of these gases at grain

boundaries of the $UO_2$, and in the gap between the cladding and the fuel once the grain boundaries have become saturated, results in swelling of the fuel. If the volume of the fuel exceeds that of the cladding, or the cladding experiences excessive strain from the swollen fuel, the cladding may rupture, resulting in reactor downtime. The solution to this issue is to improve the $UO_2$ fuel by promoting the growth of larger grains and lengthening the diffusion pathway of fission products to the grain boundaries during fission [2]. This is achieved by doping $UO_2$ with additives; the most extensively applied are $Cr_2O_3$ [1,3,4], $Al_2O_3$ [5] and a mixture thereof [1,6].

This study aimed to investigate the synthesis of $UO_2$ and $Cr_2O_3$-doped $UO_2$ by Hot Isostatic Pressing (HIP), as a potential method for fuel fabrication, and for development of analogue materials for spent nuclear fuel research. Used in a wide range of industry, HIP reduces the porosity of metals and increases the density of many ceramic materials [7]. The HIP process is based on the simultaneous application of temperature and an isostatic gas pressure (generally argon), from all directions, in a high pressure containment vessel.

## EXPERIMENTAL DETAILS

### High density Cr-doped $UO_2$ sample preparation

Chromium-doped $UO_2$ samples were synthesised by weighing appropriate concentrations of $UO_2$ and $Cr_2O_3$ (99 %, Alfa Aesar) to obtain pure $UO_2$ and $UO_2$ doped with 1200 ppm Cr. Oxide powders were homogenised by mixing in a ball mill at 30 Hz. The total mass of each sample prepared was around 18 g.

Using an uniaxial press, the obtained powders were packed into specially designed HIP canisters (316 stainless steel), which were welded closed, as shown in Figure 1. A bake-out step was performed at 300˚C for 2 h by vacuum pumping through the tube connected to the canister lid to remove air. When this had been achieved, the tube was crimped and welded to fully seal the sample in the canister.

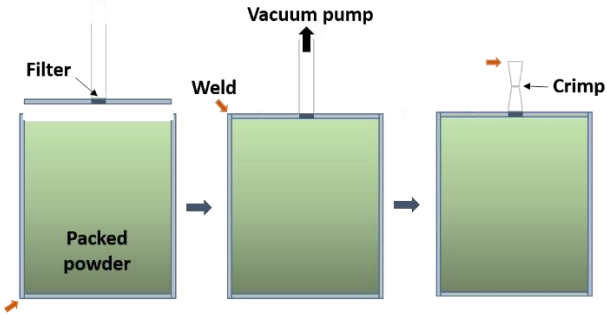


Figure 1: Schematic view of the canister packed powder and bake-out step [8].

Due to the use of α-containing materials ($^{238}U$) in the synthesis, the Active Furnace Isolation Chamber (AFIC) was designed and commissioned for processing radioactive materials using the HIP at the University of Sheffield. The risk associated with α-active contamination are mitigated through a double-filter seal containment system within the AFIC that would prevent contamination to the HIP, in the event of a release. The HIP was

ramped to a temperature of 1250˚C (5°C $min^{-1}$ below 700°C with different dwell steps and 7.5°C $min^{-1}$ up to 700°C) and a pressure of 200 MPa imposed by $Ar_{(g)}$ (1.5 MPa $min^{-1}$), and was held under these conditions for 4 hours. The temperature and pressure evolutions of the HIP cycle are detailed in Figure 2.

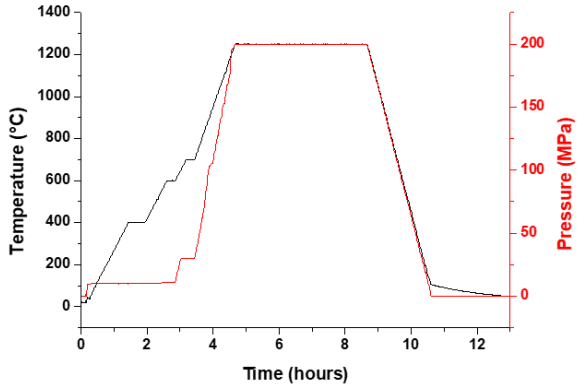


Figure 2: Temperature and pressure evolutions used for the HIP heat treatment.

After the HIP heat treatment, the canister was opened using a precision diamond saw. Photographs of the sample at the different stages of the preparation process are presented in Figure 3.

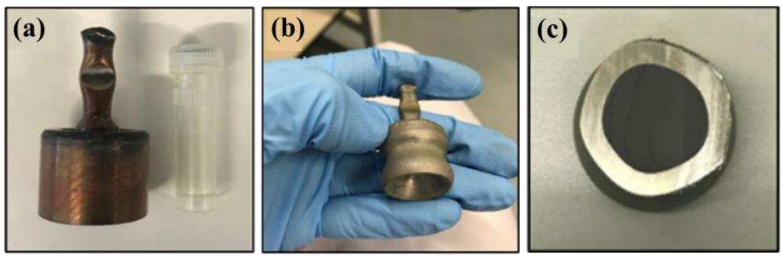


Figure 3: Photographs of (a) the baked out canister, (b) the HIPed canister, and (c) the dense sample within the canister.

## Characterisation

Scanning Electron Microscopy (SEM) images were recorded using a Hitachi TM3030 SEM equipped with a Bruker Quantax EDX operating at an accelerating voltage of 15 kV. For this purpose, samples were polished with SiC grinding papers and diamond suspensions from 9 to 1 µm. Mirror polished samples were annealed at 1100˚C for two hours under a reducing atmosphere ($H_2$ – 5%$N_2$) to reveal the microstructure. SEM micrographs of the samples recorded at low magnification were used to determine the grain size distribution, using approximately 900 grains.

Raman measurements were performed on the polished and annealed samples using a Renishaw Invia Reflex confocal spectrometer equipped with a Leica DM2500 microscope. A 514 nm (green) argon excitation laser with 1800 lines $mm^{-1}$ grating was used for a spectral acquisition between 200 and 750 $cm^{-1}$. These configurations were sufficient to

allow 2-3 $cm^{-1}$ spectral resolution. The Raman data were obtained with an acquisition time of 60 s after 5 accumulations using the x100 objective.

Powder X-ray Diffraction (XRD) patterns were acquired using a Bruker D2 Phaser diffractometer in reflection mode at 30 kV and 10 mA with Cu $K\alpha_1$ radiation ($\lambda$ = 1.5418 Å). For this purpose, the HIP canister was removed from the sample using a diamond saw, and a fragment of the sample was released and ground into a fine powder. Data were collected on powders between $20 < 2\theta < 100^\circ$ at $4^\circ$ $min^{-1}$ and a step size of $0.02^\circ$. Le Bail analysis of phases identified in the diffraction patterns was performed using the refinement software Topas (Bruker) [9].

The density of the samples was determined by Archimedes measurements. Ten measurements per sample were recorded using a density kit mounted on the precision balance. The apparent density, $d_{archi}$ (g $cm^{-3}$), was evaluated and compared to the calculated density of $UO_2$ ($d_{calc.}$ = 10.97 g $cm^{-3}$) to determine the theoretical density of the samples.

## RESULTS AND DISCUSSION

### Morphological characterisation

Polished and annealed $UO_2$ and Cr-doped $UO_2$ are shown in Figure 4a and b, respectively. In general, the samples appeared dense with few pores apparent.

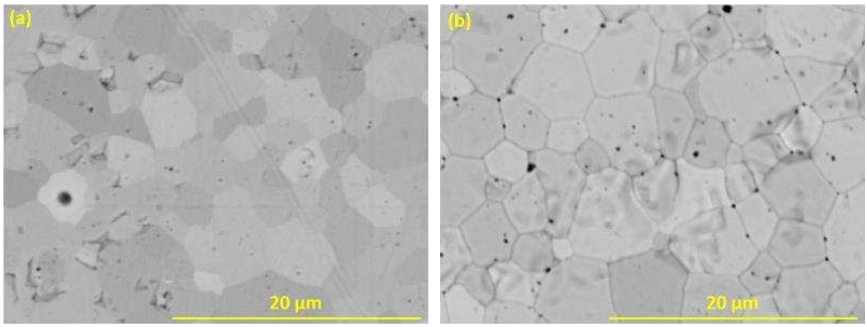


Figure 4: SEM micrographs of the samples prepared by HIP sintering: (a) $UO_2$ and (b) Cr-doped $UO_2$.

The main difference in the microstructure between the two samples was the presence of black particles in the Cr-doped $UO_2$, mainly located within the grain boundaries (Figure 5a). Analysis by EDX (Figure 5b) confirmed that these were Cr-containing. The presence of such particles may be due to non-incorporation of Cr in the $UO_2$ structure, or the precipitation of $Cr_2O_3$ once limit of solubility of Cr in $UO_2$ has been reached.

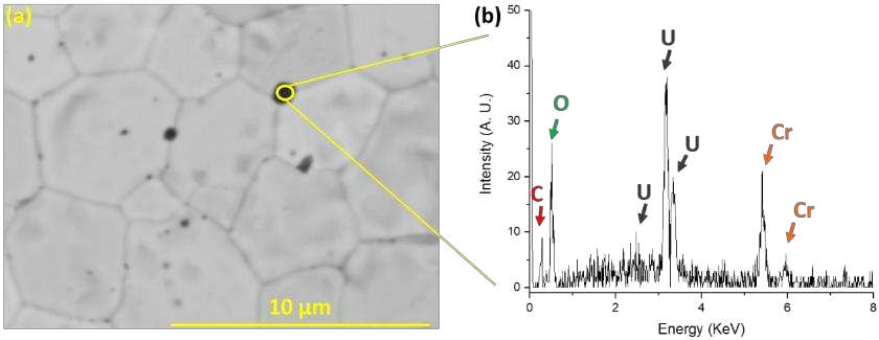


Figure 5: (a) SEM micrographs used for EDX analyses performed on 1200 ppm Cr-doped $UO_2$ sample, (b) EDX spectrum of the yellow circled area showing the presence of Cr. The EDX spectrum of the bulk matrix is the same as in (b), but without Cr.

The grain size and the density of the samples are given in Table 1, and the grain size distribution is presented in Figure 6. The addition of 1200 ppm Cr did not significantly influence the $UO_2$ grain size when compared to the un-doped sample. This is in contrast to previous studies of Cr-doped $UO_2$, which tend to have significantly increased grain size when compared to $UO_2$. For example, Arborelius *et al.* [1] evidenced an increase in grain size from 11 µm in $UO_2$ to 42 µm when $UO_2$ was doped with of 1000 ppm of $Cr_2O_3$; both were sintered at 1800˚C for 14h in a $H_2/CO_2$ atmosphere. Similarly, Bourgeois *et al.* [3] showed that a grain size of ~75 µm could be achieved for ~700 ppm Cr-doped $UO_2$ sintered at 1700˚C, when sintering was performed in the presence of $H_2$ + 1 vol.% $H_2O$. The sintering atmosphere clearly plays an important role in the incorporation of Cr into the $UO_2$ structure and, since the atmosphere for the HIP synthesis performed in this study was identical for both doped and un-doped samples (non-hydrous, inert atmosphere (Ar) and reducing conditions imposed by the stainless steel canister [10]), it is perhaps unsurprising that the microstructures obtained did not differ significantly.

Table 1: Composition, densification rates from geometric measurements (%) and grains size (µm) of un-doped $UO_2$, 1200 ppm Cr-doped $UO_2$.

| Sample composition | Archimedes density (%) | Grains size (µm) |
|---|---|---|
| $UO_2$ | 96.7 ± 1.0 | 3.4 ± 0.2 |
| $UO_2$ + 1200 ppm Cr | 96.6 ± 1.0 | 4.0 ± 0.3 |

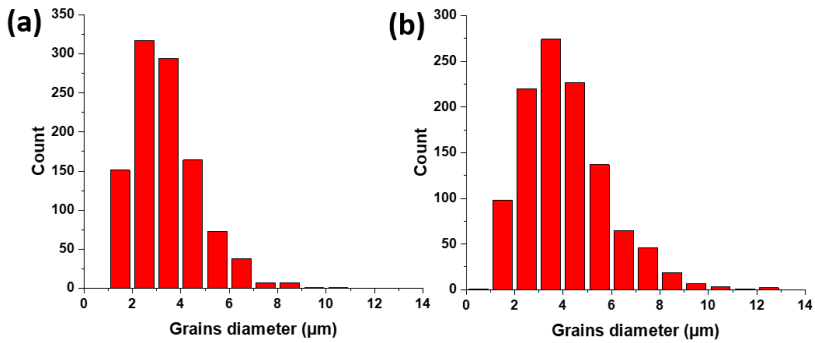


Figure 6: Grain size distribution measured by SEM image analysis for (a) un-doped $UO_2$, (b) 1200 ppm Cr-doped $UO_2$.

The Archimedes density measurements presented in Table 1 show that there was no difference in the final density of the $UO_2$, with or without Cr (96.7 ± 1.0 % for $UO_2$ and 96.6 ± 1.0 % for 1200 ppm Cr-doped $UO_2$), confirming the low influence of Cr on the $UO_2$ microstructure prepared through the HIP method. However, in comparison with $UO_2$ samples prepared *via* classic sintering at 1700˚C for 8h under 95 %$H_2$ – 5 %$N_2$ in a tube furnace, which gave a theoretical density of 90%, the HIP sample was more dense, due to the isostatic argon pressure applied during synthesis that eliminates porosity during sintering.

## Chemical characterisation

XRD patterns of both samples are presented in Figure 7. These patterns confirmed that the samples crystallised in the fluorite structure (space group $Fm\bar{3}m$), with a crystalline structure characteristic of $UO_2$ [11].

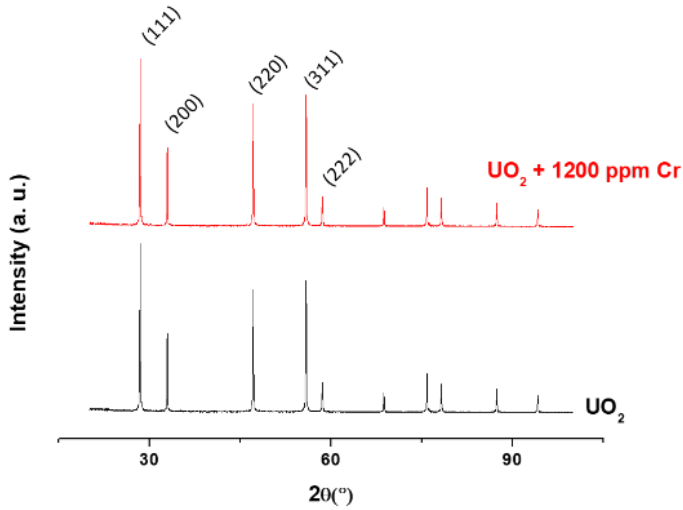


Figure 7: Powder X-ray diffraction patterns of un-doped $UO_2$ (black curve) and 1200 ppm Cr-doped $UO_2$ (red curve) samples.

The lattice parameter of the un-doped $UO_2$ sample was determined to be $a$ = 5.4738(5) Å, in agreement with previously reported values for $UO_2$ synthesised via dry synthesis methods ($a$ = 5.47127(8) Å) [12]. The lattice parameter for the 1200 ppm Cr-doped $UO_2$ was determined to be $a$ = 5.4772(6) Å. The slightly increased lattice parameter induced by Cr-doping is somewhat unexpected since the radius of the $Cr^{3+}$ ion (0.615 Å) is smaller than that of $U^{4+}$ (1.03 Å); therefore if Cr were incorporated in the $UO_2$ lattice, a decrease of the lattice parameter of $UO_2$ should be expected [13]. Such an increase might be due to incorporation of Cr into $UO_2$ in a different valence state, as predicted by [14]. Indeed, the ionic radii of $Cr^{1+}$ and $Cr^{2+}$ are 1.09 Å and 0.89 Å, respectively; the presence of a reduced form of Cr, induced by the reducing conditions during the HIP synthesis, may result in an increase of the lattice size.

Analysis of the samples by Raman spectroscopy (Figure 8), showed a main peak at 445 $cm^{-1}$ relating to the symmetric $T_{2g}$ vibration mode for $UO_2$ [15], with a second peak

observed at 575 $cm^{-1}$, known as the Longitudinal optical (LO) band [16]. The LO band is characteristic of the presence of crystalline defects in the sample. In Figure 8b, the area and height ratios between the $T_{2g}$ and the LO bands, which can be described as a defect ratio, indicate that there was a small increase, albeit within error, in the quantity of defects in $UO_2$ when Cr was added. This may be associated with the substitution of Cr for $U^{4+}$ in the $UO_2$ lattice and the associated development of structural defects, such as oxygen vacancies, oxygen interstitials, $U^{5+}$, and changes in cubic cell symmetry. The presence of such defects may also be responsible for the observed XRD results, however, further analysis is required to verify the nature of the defects.

It is worth noting that the Cr doping was at the ppm-level and, according to EDX mapping and the small change in the lattice parameter, most of the Cr was segregated near the GB areas. The Raman measurements were performed at the centre of the grains, where Cr had little effect compared to the grain boundaries. Thus, the dopant, does at a certain extent, modify the crystalline structure but the disorder associated with Cr-incorporation is relatively low/not sufficient enough to cause a significant change in the LO-band. However, the small increase observed, though it is within the error bars, do indicate the presence of a low defect concentration, which is also responsible for the change in the lattice parameter.

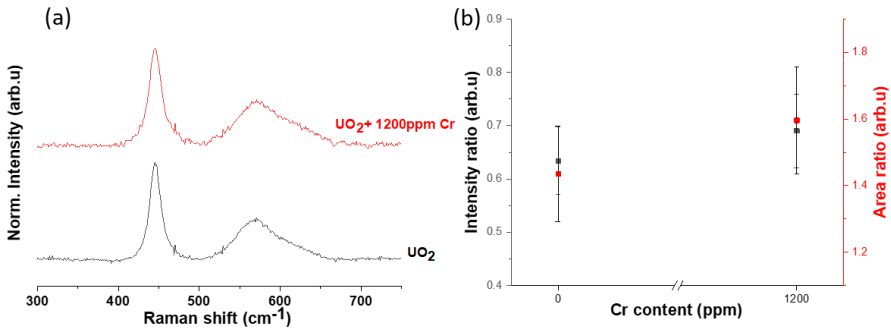


Figure 8: (a) Raman spectroscopy patterns of un-doped $UO_2$ and Cr-doped $UO_2$; and (b) showing the height ratio (■) and the area ratio (●) between $T_{2g}$ and LO bands (obtained from (a)) for each sample.

## CONCLUSION

High density $UO_2$ samples, with and without the addition of Cr, were synthesized by Hot Isostatic Pressing. Microstructural characterization evidenced no difference in the grain size or density of the materials, which is hypothesized to result from the atmosphere conditions and the temperature imposed by the HIP process. These conditions may also have promoted the formation of reduced Cr within $UO_2$, as inferred from lattice parameter values; further analysis by oxidation state sensitive techniques (e.g. XANES) is required to confirm this. The presence of particles of $Cr_2O_3$ at grain boundaries suggests that 1200 ppm of Cr exceeds the solubility limit of Cr in $UO_2$. In comparison with classically sintered $UO_2$, the density of the HIPed material was greater, as expected for this technique.

## ACKNOWLEDGEMENTS

We wish to acknowledge funding for this research from the European Commission Horizon 2020 Research and Training Programme, DISCO, of the European Atomic Energy Community (EURATOM), under grant agreement number 755443. CLC wishes to thank EPSRC for the award of an Early Career Fellowship under grant agreement EP/N017870/1, and the DISTINCTIVE programme (EP/L014041/1) radioactive fund. RM wishes to acknowledge EPSRC for funding under the UK-US Nuclear Energy University Programme (EP/R006075/1). This research was performed at the MIDAS Facility, at the University of Sheffield, which was established with support from the UK Department of Energy and Climate Change.

## REFERENCES

[1] J. Arborelius, K. Backman, L. Hallstadius, J. Nilsson, B. Rebensdorff, G. Zhou, R. Löfström, G. Rönnberg, J. Arborelius, K. Backman, L. Hallstadius, J. Nilsson, B. Rebensdorff, G. Zhou, K. Kitano, J. Nilsson, Advanced Doped $UO_2$ Pellets in LWR Applications, 3131 (2012). doi:10.1080/18811248.2006.9711184.

[2] R. Yuda, H. Harada, T. Hosokawa, K. Une, S. Kashibe, S. Shimizu, T. Kubo, Effects of pellet microstructure on irradiation behavior of $UO_2$, J. Nucl. Mater. 248 (1997) 262–267.

[3] L. Bourgeois, P. Dehaudt, C. Lemaignan, A. Hammou, Factors governing microstructure development of $Cr_2O_3$-doped $UO_2$ during sintering, J. Nucl. Mater. 297 (2001) 313–326. doi:10.1016/S0022-3115(01)00626-2.

[4] A. Leenaers, L. De Tollenaere, C. Delafoy, S. Van den Berghe, On the solubility of chromium sesquioxide in uranium dioxide fuel, J. Nucl. Mater. 317 (2003) 62–68. doi:10.1016/S0022-3115(02)01693-8.

[5] D.. Kim, Effect of small amounts of aluminium doping on the grain growth of a $UO_2$ pellet, Trans. Korean Nucl. Soc. Spring Meet. (2006).

[6] M.W.D. Cooper, D.J. Gregg, Y. Zhang, G.J. Thorogood, G.R. Lumpkin, R.W. Grimes, S.C. Middleburgh, Formation of (Cr, Al)$UO_4$ from doped $UO_2$ and its influence on partition of soluble fission products, J. Nucl. Mater. 443 (2013) 236–241. doi:10.1016/j.jnucmat.2013.07.038.

[7] H. V Atkinson, S. Davies, Fundamental Aspects of Hot Isostatic Pressing: An Overview, m (2000).

[8] S. M. Thornber. The Development of Zirconolite Glass-Ceramics for the Disposition of Actinide Wastes. PhD Thesis, The University of Sheffield (2018).

[9] D. Balzar, Voight-Function Model in Diffraction line Broadening Analysis, Microstruct. Anal. from Diffr. (1999).

[10] E.R. Vance, M.W.A. Stewart, S.A. Moricca, Progress at ANSTO on SYNROC, J. Aust. Ceram. Soc., 50 (2014) 38–48.

[11] T. Tsuji, M. Iwashita, T. Yamashita, K. Ohuchi, Effect of cations on lattice constants of $(M_yU_{1-y})O_{2.00}$ (M = Pu, Th, La) at low doped cation concentrations, J. Nucl. Mater. 273 (1998) 391–394.

[12] G. Leinders, T. Cardinaels, K. Binnemans, M. Verwerft, Accurate lattice parameter measurements of stoichiometric uranium dioxide, J. Nucl. Mater. 459 (2015) 135–142. doi:10.1016/j.jnucmat.2015.01.029.

[13] T. Cardinaels, K. Govers, B. Vos, S. Van Den Berghe, M. Verwerft, L. De Tollenaere, G. Maier, C. Delafoy, Chromia doped $UO_2$ fuel: Investigation of the lattice parameter, J. Nucl.

Mater. 424 (2012) 252–260. doi:10.1016/j.jnucmat.2012.02.025.

[14] M.W.D. Cooper, C.R. Stanek, D.A. Andersson, The role of dopant charge state on defect chemistry and grain growth of doped $UO_2$, Acta Mater. 150 (2018) 403–413. doi:10.1016/j.actamat.2018.02.020.

[15] L. Desgranges, G. Baldinozzi, G. Rousseau, J. Ni, Neutron Diffraction Study of the in situ Oxidation of $UO_2$, (2009) 7585–7592. doi:10.1021/ic9000889.

[16] R. Mohun, L. Desgranges, J. Léchelle, P. Simon, G. Guimbretière, A. Canizarès, F. Duval, C. Jegou, M. Magnin, N. Clavier, N. Dacheux, C. Valot, R. Vauchy, Charged defects during alpha-irradiation of actinide oxides as revealed by Raman and luminescence spectroscopy, Nucl. Inst. Methods Phys. Res. B. 374 (2016) 67–70. doi:10.1016/j.nimb.2015.08.003.